NEURAL REGENERATION RESEARCH
www.nrronline.org

Research Article

Neural stem cell-derived exosome as a nano-sized carrier for BDNF delivery to a rat model of ischemic stroke

Zhi-Han Zhu[1], Feng Jia[2], Waqas Ahmed[1], Gui-Long Zhang[3], Hong Wang[1], Chao-Qun Lin[1], Wang-Hao Chen[4], Lu-Kui Chen[1, 2, *]

https://doi.org/10.4103/1673-5374.346466
Date of submission: December 20, 2021
Date of decision: January 29, 2022
Date of acceptance: March 4, 2022
Date of web publication: June 2, 2022

From the Contents

Graphical Abstract

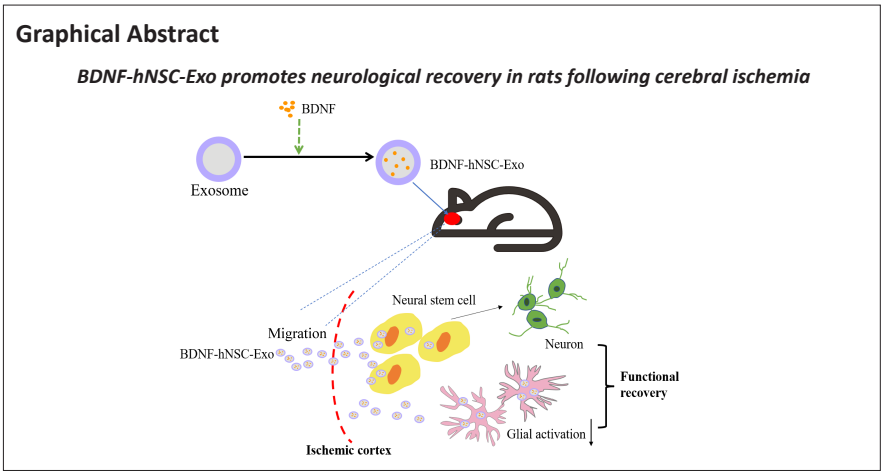

Abstract

Our previous study demonstrated the potential therapeutic role of human neural stem cell-derived exosomes (hNSC-Exo) in ischemic stroke. Here, we loaded brain-derived neurotrophic factor (BDNF) into exosomes derived from NSCs to construct engineered exosomes (BDNF-hNSC-Exo) and compared their effects with those of hNSC-Exo on ischemic stroke both *in vitro* and *in vivo*. In a model of H_2O_2-induced oxidative stress in NSCs, BDNF-hNSC-Exo markedly enhanced cell survival. In a rat middle cerebral artery occlusion model, BDNF-hNSC-Exo not only inhibited the activation of microglia, but also promoted the differentiation of endogenous NSCs into neurons. These results suggest that BDNF can improve the function of NSC-derived exosomes in the treatment of ischemic stroke. Our research may support the clinical use of other neurotrophic factors for central nervous system diseases.

Key Words: brain-derived neurotrophic factor; exosome; inflammation; ischemic stroke; neural stem cell; neurogenesis; neurological recovery; transplantation

Introduction

Stroke has become a tremendous threat to human health and has placed an enormous burden on health care systems worldwide (Leira et al., 2020). A systematic analysis of the 2019 Global Burden of Disease Study showed a 70.0% increase in the absolute number of incident strokes and a 43.0% increase in stroke deaths worldwide from 1990 to 2019 (Ma et al., 2021). Ischemic stroke accounted for 62.4% of all strokes in 2019 and has remained the largest proportion of all incident strokes. Tissue-type plasminogen activator is the only effective drug for stroke and must be administered within 4.5 hours of stroke. However, because of the limited therapeutic window (Goldstein, 2007), only a small percentage of individuals can benefit from tissue-type plasminogen activator therapy (Hughes et al., 2020; Marko et al., 2020). Integrated neuroprotective techniques to minimize ischemic injury remain scarce (Zhang et al., 2016).

Neurotrophic factors are a group of proteins that are vital for the development, growth, survival, and differentiation of the nervous system (Muheremu et al., 2021). Brain-derived neurotrophic factor (BDNF) is the most abundant and widely distributed neurotrophic factor in the nervous system. BDNF promotes cell differentiation, cell growth, synaptogenesis, and neurogenesis in the nervous system by stimulating its tropomyosin receptor kinase B (Hao et al., 2021; Xiong et al., 2021). Importantly, BDNF was shown to exhibit numerous neuroprotective properties in post-ischemic and traumatic brain injury (Li et al., 2021). Studies demonstrated that BDNF promotes the proliferation of endogenous neural stem cells (NSCs) and the regeneration of nerve axons in rats with spinal cord injury (Huang et al., 2021). However, exogenous administration of neurotrophic factors for stroke treatment is limited by their poor half-life, lack of blood-brain barrier permeability, and rapid degradation (Yuan et al., 2017; Naqvi et al., 2020).

Exosomes are small extracellular vesicles 30–200 nm in size that are secreted by various cell types and contain a variety of proteins, microRNAs, and other macromolecules (Zhang and Chopp, 2016b; Chen et al., 2020). Compared with conventional carriers (such as liposomes), exosomes offer a number of advantages, including minimal immunogenicity (Fang et al., 2020), minimal toxicity (Fu et al., 2019), biocompatibility (Wu et al., 2021), high circulation stability (Kim et al., 2020), and biological barrier permeability (Feng et al., 2021), making them ideal drug delivery vehicles (Xu et al., 2021). Recent studies have shown that NSCs exert therapeutic effects by releasing exosomes (Vogel et al., 2018). Zhong et al. (2020) found that NSC-derived exosomes (NSC-Exo) significantly promoted angiogenesis, constricted the spinal cavity, and improved motor function in spinal cord injury mice. Another study showed that miR-9, a key regulator of neurogenesis, was highly enriched in NSC-Exo exosomes, and miR-9-enriched NSC-Exo promoted the differentiation of NSCs into neurons and astrocytes (Yuan et al., 2021).

In this study, we loaded BDNF into human NSC (hNSC)-derived exosomes to construct BDNF-hNSC-Exo and investigated the potential application of BDNF-hNSC-Exo in ischemic stroke both *in vitro* and *in vivo*.

[1]Department of Neurosurgery, School of Medicine, Southeast University, Nanjing, Jiangsu Province, China; [2]Department of Neurosurgery, Neuroscience Center, Cancer Center, Integrated Hospital of Traditional Chinese Medicine, Southern Medical University, Guangzhou, Guangdong Province, China; [3]Department of Neurosurgery, The Second Affiliated Hospital of Guangzhou Medical University, Guangzhou, Guangdong Province, China; [4]Department of Neurosurgery, Shanghai Ninth People's Hospital, Shanghai Jiao Tong University School of Medicine, Shanghai, China
***Correspondence to:** Lu-Kui Chen, MD, neuro_clk@hotmail.com.
https://orcid.org/0000-0002-8075-8369 (Lu-Kui Chen)

Funding: *This work was supported by the National Natural Science Foundation of China, No. 81671819 (to LKC), and the Natural Science Foundation of Guangdong Province, Nos. 2021A1515010001 and 2019A1515012103 (both to LKC).*
How to cite this article: *Zhu ZH, Jia F, Ahmed W, Zhang GL, Wang H, Lin CQ, Chen WH, Chen LK (2023) Neural stem cell-derived exosome as a nano-sized carrier for BDNF delivery to a rat model of ischemic stroke. Neural Regen Res 18(2):404-409.*

Methods

hNSC culture and differentiation

hNSCs were purchased from the Shanghai Binsui Biotechnology Co., Ltd (Shanghai, China, Cat# BSC-5310479662-01). hNSCs were dissociated into single cells with Accutase Dissociation Substance (MilliporeSigma, Burlington, MA, USA, Cat# A6964) and cultured in DMEM/F12 (Gibco, Carlsbad, CA, USA, Cat# 12634) supplemented with 2% B27 (Gibco, Cat# 17504), 20 ng/mL basic fibroblast growth factor (PeproTech, Cranbury, NJ, USA, Cat# AF-100-18C), 20 ng/mL epidermal growth factor (PeproTech, Cat# AF-100-15-100), 2 nM glutamate (MilliporeSigma, Cat# 1446600), 2 μg/mL heparin sodium (MilliporeSigma, Cat# H3149), and 1% penicillin-streptomycin (Gibco, Cat# 15070063) in a 5% CO_2 humidified atmosphere at 37°C. To stimulate the differentiation-inducing environment *in vivo*, hNSCs were cultured in DMEM/F12 (Gibco, Cat# 12634) supplemented with 2% B27 (Gibco, Cat# 17504), 0.5% fetal bovine serum (Gibco, Cat# 10100147C), and 1× N2 supplement (Gibco, Cat# 17502048). After 5–7 days of differentiation induction, the number of NSCs that differentiated into neurons and astrocytes was assessed. hNSCs at passage 3 were cultured in stem cell medium or differentiation medium.

Immunofluorescence was used for the identification of hNSCs using antibodies against NSC-related markers mouse monoclonal anti-Nestin (1:200, Abcam, Cat# ab18102, RRID: AB_444246) and rabbit monoclonal anti-Sox2 (1:50, Abcam, Cat# ab93689, RRID: AB_10562630) and differentiation-related markers rabbit monoclonal anti-class III β-tubulin (Tuj1; 1:500, Abcam, Cat# ab52623, RRID: AB_869991), mouse monoclonal anti-glial fibrillary acidic protein (GFAP; 1:50, Abcam, Cat# ab4648, RRID: AB_449329), and rabbit monoclonal anti-myelin oligodendrocyte glycoprotein (MOG; 1:500, Abcam, Cat# ab109746, RRID: AB_10863418). Secondary antibodies included Alexa Fluor® 488-conjugated goat anti-rabbit antibody (1:500, Abcam, Cat# ab150077, RRID: AB_2630356) and goat anti-mouse antibody (1:300, Abcam, Cat# ab150113, RRID: AB_2576208) and Alexa Fluor® 555-conjugated goat anti-mouse (1:500, Abcam, Cat# ab150118, RRID: AB_2714033) and goat anti-rabbit antibodies (1:400, Abcam, Cat# ab150078, RRID: AB_2722519).

Exosome isolation and identification

Exosomes derived from hNSCs were isolated as previously described (Zhang et al., 2018, 2020). Briefly, the hNSC culture medium was harvested in sterile conditions and centrifuged at 3000 × *g* for 30 minutes to eliminate cellular debris. The supernatant was filtrated with a 0.22 μm membrane (MilliporeSigma, Cat# SLGP033RB), and the filtrate was centrifuged at 110,000 × *g* for 2 hours at 4°C. Finally, the exosome pellets were resuspended in 100 μL PBS and immediately stored at –80°C.

The exosome solution was fixed on a copper mesh (MilliporeSigma, Cat# G4776), negatively stained with phosphotungstic acid (MilliporeSigma, Cat# P4006), and then air-dried for morphological observation using a transmission electron microscope (TEM) (Gatan, Pleasanton, CA, USA). NTA was done by ZetaView PMX 110 system (Particle Metrix, Meerbusch, Germany) was used to measure the hydrodynamic size and concentration of hNSC-Exo and BDNF-hNSC-Exo.

Western blotting was used to evaluate exosome surface markers using specific antibodies: rabbit anti-human heat shock protein 70 (HSP70) monoclonal antibody (1:3000, Abcam, Cat# ab45133, RRID: AB_733035), mouse monoclonal anti-tumor susceptibility 101 (TSG101; 1:2000, Thermo Fisher Scientific, Waltham, MA, USA, Cat# MA1-23296, RRID: AB_2208088), mouse monoclonal anti-CD81 (1:3000, Abcam, Cat# ab109201, RRID: AB_10866464), and calnexin (1:20,000, Abcam, Cat# ab92573, RRID: AB_10563673).

Exosome uptake by hNSCs

Fluorescent labeling of hNSC-Exo and BDNF-hNSC-Exo was performed using the PKH67 Green Fluorescent Cell Linker Kit (MilliporeSigma, Cat# MINI67) following the manufacturer's instructions. PKH67 and 0.5 mL Diluent C were mixed, added to premixed 0.5 mL Diluent C and 50 μL exosomes, and incubated for 4 minutes. Staining was stopped by adding 1 mL of 0.5% BSA (Servicebio, Wuhan, Hubei, China, Cat# G5001). Unbound dye was removed by ultracentrifugation at 120,000 × *g* for 1 hour at 4°C; the sample was washed three times with PBS and resuspended. Labeled exosomes were incubated with hNSCs for 48 hours. The cells were fixed with 4% paraformaldehyde, and nuclei were stained with DAPI (Beyotime, Nanjing, Jiangsu, China, Cat# C1002) for 5 minutes. The uptake of PKH67-labeled hNSC-Exo or BDNF-hNSC-Exo by hNSCs was observed under a fluorescence microscope (Nikon, Tokyo, Japan, Cat# Ts2R).

Loading of BDNF into exosomes

BDNF was co-incubated with hNSC-Exo for 24 hours followed by loading of BDNF into exosomes using Exo-Fect reagent (System Biosciences, San Francisco, CA, USA, Cat# EXFT10A-1). The isolated exosomes were mixed with Exo-Fect reagent and BDNF protein (Proteintech, Wuhan, Hubei, China, Cat# Ag11329) for 10 minutes at 37°C following the manufacturer's instructions, and the reaction was stopped by adding 30 μL of ExoQuick-TC reagent (System Biosciences, Cat# EXOTC10A-1) and incubation on ice for 30 minutes. The sample was then centrifuged at 14,000 × *g* for 3 minutes at 4°C.

Immunofluorescence

The differentiation ability of NSCs into neurons was detected by immunofluorescence staining. hNSCs were seeded in 24-well culture plates at a density of 3×10^4 cells/mL medium/well and treated with 500 μM H_2O_2 (MilliporeSigma, Cat# 88597) solution for 5 hours. Cells were treated with PBS, hNSC-Exo, or BDNF-hNSC-Exo (100 μg/mL) for 72 hours and then coated with anti-Tuj1, a marker for neurons; 1:500, Abcam, Cat# ab52623, RRID: AB_869991) dissolved in blocking suspension. Following the addition of Alexa Fluor® 555-conjugated goat secondary antibodies (1:400, Abcam, Cat# ab150078, RRID: AB_2722519) and DAPI (Beyotime, Cat# C1002), the specimens were observed under a fluorescence microscope.

Cell Counting Kit-8 assay

The cell viability of hNSCs was determined by Cell Counting Kit-8 (CCK-8) assay (Yeasen, Shanghai, China, Cat# 40203ES60). hNSCs were seeded in 96-well culture plates at a density of 1×10^4 cells/100 μL medium/well and treated with a 500 μM solution H_2O_2 for 5 hours to stimulate the process of cellular oxidative injury, prompting programmed cell death. The samples were then treated with 100 μg/mL PBS, hNSC-Exo, or BDNF-hNSC-Exo (100 μg/mL) at 37°C for 4 hours, 1 day or 2 days. Next, 10 μL of CCK-8 solution was added to each well and the sample was incubated at 37°C for 4 hours. The absorbance of each well at 450 nm was measured using a microplate reader (Thermo Fisher Scientific, Cat# MK3).

Terminal deoxynucleotidyl transferase dUTP nick end labeling staining

Apoptosis was measured using the CF488 TUNEL (terminal deoxynucleotidyl transferase dUTP nick end labeling) Cell Apoptosis Detection Kit (Servicebio, Cat# G1504). Briefly, hNSCs were fixed with 4% paraformaldehyde (Servicebio, Cat# G1101), washed three times with PBS, covered with 50 μL Equilibration Buffer and incubated at room temperature for 10 minutes, followed by incubation in TdT incubation buffer (Servicebio, Cat# G1504-1) at 37°C for 60 minutes. The hNSCs were incubated with DAPI for 5 minutes for nuclear staining. Three fields of view were randomly selected under the fluorescence microscope and TUNEL-positive cells were counted by two independent observers. The TUNEL-positive rate (%) was calculated as: TUNEL-positive cells/total number of cells × 100.

Quantitative reverse transcription-polymerase chain reaction

TRIZOL reagent (Thermo Fisher Scientific, Cat# 15596) was used to isolate total RNA from hNSCs following the company's instructions. Total RNA (500 ng) was reverse transcribed to cDNA using the HiScript® 1st Strand cDNA Synthesis Kit (Vazyme, Nanjing, Jiangsu, China, Cat# R111-01). Amplification reactions were performed in a 20 μL reaction volume using SYBR Green (Vazyme, Cat# Q341-02) in a Roche LightCycler 96 Sequence Detection System (Roche, Basel, Switzerland). The reaction conditions were as follows: pre-denaturation at 95°C for 30 seconds, followed by 40 cycles of amplification at 95°C for 15 seconds and 60°C for 30 seconds. The relative expression of mRNA was calculated using the $2^{-\Delta\Delta Cq}$ method and normalized using GAPDH mRNA. Each experiment was repeated three times. Quantitative reverse transcription-polymerase chain reaction primers were designed using Primer Premier 5 software (Premier, Palo Alto, CA, USA). The primers were as follows: Tuj1: forward 5′-CGT CCA CAG TTC TGG GAA GTC A-3′, reverse 5′-CGG GAT ACT CCT CAC GC ACC T-3′; GAPDH: forward 5′-TTT GGT ATC GTG GAA GGA-3′, reverse 5′-GAG TGG GTG TCG CTG TT-3′.

Establishment of transient middle cerebral artery occlusion model rats and exosome treatment

Healthy adult male Sprague-Dawley rats (*n* = 60, aged 8 weeks, weight 250–280 g, specific-pathogen-free grade) were purchased from Hangzhou Medical College (Hangzhou, Zhejiang, China, license No. SCXK (Zhe) 2019-0002)). All animals were maintained under standardized conditions at 28°C and a 12-hour light/dark cycle, with free access to water and food. All animal trials were approved by the Institutional of Animal Care and Use Committee at the Medical School of Southeast University (approval No. SYXK (Su) 2021-0022)) on April 5, 2021 and were performed in accordance with the ARRIVE 2.0 guidelines (Animal Research: Reporting of *In Vivo* Experiments) (Percie du Sert et al., 2020).

Middle cerebral artery occlusion (MCAO) surgery was performed as previously described (Zhang et al., 2018). Briefly, rats were anesthetized with 1% pentobarbital sodium (MilliporeSigma, 25 mg/kg). The subcutaneous tissue and muscle were bluntly dissected with vascular forceps, and the common carotid, external, and internal carotid arteries were gently dissected with microtweezers without damaging the vagus nerve. A nylon thread (Cinon, Beijing, China, Cat# A5-243605) was inserted into the right (supine) common carotid artery; the blood flow was blocked as the distal end of the nylon thread was injected into the internal carotid artery. The nylon thread was removed after 1.5 hours of ischemia, and the wound was sutured closed. The body temperature of the rats was closely monitored during the operation until the rats were awake. Following the Zea-Longa score (Zhang et al., 2019), 1–3 points were determined as successful modeling, and a Longa score of 2 was used for subsequent experiments.

At 72 hours after MCAO, rats (*n* = 15/group) were randomly injected with PBS, hNSC-Exo, and BDNF-hNSC-Exo (5×10^9 granules in 10 μL PBS/rat) via stereo-tactical insertion through the striatum of the ischemic hemisphere to promote nerve regeneration at 72 hours after MCAO. For the stereotaxic position, the bregma was taken as the zero point, and the injection sites were anteroposterior = 0.5 mm, mediolateral = 3 mm, dorsoventral = 4.5 mm (Paxinos and Watson, 2009). Rats were continuously injected with 5-bromo-2′-deoxyuridine (BrdU, MilliporeSigma, Cat# B5002) 3 days before sacrifice by intraperitoneal injection to assess the proliferation or differentiation of endogenous NSCs.

Behavioral tests
To test the neuroprotective effects of BDNF-hNSC-Exo *in vivo*, the MCAO model rats were subjected to behavioral evaluation. Rats underwent three days of behavioral training before MCAO. Tests were performed before MCAO and 1, 3, 7, 14, and 28 days after transplantation by two research assistants who were blinded to the groups.

For the rotator test, a motorized rotating rod (RWD, Shenzhen, Guangdong, China) was used to test the sensorimotor function of rats. Rats were placed on a rod that accelerated from 4 r/min to 40 r/min in 5 minutes, and the stick time of each rat was recorded.

The postural reflex examination assesses the vulnerability to brain and striatum damage on a scale of 0 to 10. For the postural reflex test, the rat was placed on a smooth surface or suspended in the air, and the rat's behavior and muscle strength were evaluated. A higher score suggested that the animal had a more significant behavioral problem.

Neurological function was determined using the modified neurological severity score (mNSS) test. Scores ranged from 0 to 18 (normal score, 0; maximum score, 18). An mNSS score of 13–18 indicated severe damage, 7–12 indicated moderate damage, and 1–6 indicated mild damage. A higher score indicates more severe damage.

TTC staining
Rat brains were rapidly removed on the 28th day after transplantation; brain tissue was sliced into six equidistant slices (n = 6 each rat) and stained with a 2% 2,3,5-triphenyltetrazolium chloride (Servicebio, Cat# G1017) solution. Pictures were analyzed using ImageJ software. To eliminate the effect of brain swelling in the infarcted cerebral hemisphere, infarct size was calculated by subtracting the area of non-infarcted tissue in the ipsilateral hemisphere from the normal contralateral hemisphere area, and then the entire infarction amount of rats per superposition was computed (Arumugam et al., 2006).

Immunostaining of brain slices
Rat were transcardially perfused with PBS and 4% paraformaldehyde. Rat brain tissues were embedded with optimal cutting temperature compound (Servicebio, Cat# G6059) and cut into coronal sections of 10–20 μm thickness using a CM3050 S vibratome (Leica, Hesse, Germany). Sections were washed three times with PBS, incubated with Triton X-100 (MilliporeSigma, Cat# 93443) for 30 minutes and blocked in 10% donkey serum (MilliporeSigma, Cat# D9663) for 1 hour. The slides were incubated overnight at 4°C with diluted primary antibodies: rabbit polyclonal anti-BrdU (1:500, Abcam, Cat# ab152095, RRID: AB_2813902), mouse monoclonal anti-GFAP (1:50, Abcam, Cat# ab4648, RRID: AB_449329), mouse monoclonal anti-Tuj1 (1:500, Proteintech, Cat# 66375-1-Ig, RRID: AB_2814998), and rabbit polyclonal anti-Iba-1 (1:300, Proteintech, Cat# 10904-1-AP, RRID: AB_2224377). The next day, the sections were washed three times with PBS and incubated with Alexa Fluor® 488-conjugated anti-mouse IgG (1:300, Abcam, Cat# ab150113, RRID: AB_2576208) or Alexa Fluor® 555-conjugated anti-rabbit IgG (1:400, Abcam, Cat# ab150078, RRID: AB_2722519) at room temperature for 1hour. Nuclei were stained with DAPI for 5 minutes. Three fields of view were randomly selected under a fluorescence microscope, and the positive rates of BrdU/Tuj1, BrdU/GFAP, and Iba-1 were evaluated by two independent and uniform observers. The positive rate (%) was calculated as: positive cells (BrdU/Tuj1, BrdU/GFAP or Iba-1)/total number of cells × 100.

Western blotting
Total proteins were obtained from hNSCs or cerebral ischemic tissue, and protein concentration was tested using a BCA protein content detection kit (Beyotime, Cat# P0012S). Protein samples (approximately 20 μg) were boiled at 100°C for 5–10 minutes, separated by electrophoresis on a 10% or 12% sodium dodecyl sulfate polyacrylamide gel, and transferred onto polyvinylidene fluoride membranes. The membranes were blocked with 5% nonfat milk for 1 hour, and then incubated overnight at 4°C with diluted primary antibodies: rabbit polyclonal anti-BDNF (1:1000, Proteintech, Cat# 28205-1-AP, RRID: AB_2818984), rabbit polyclonal anti-β-actin (1:2500, Proteintech, Cat# 20536-1-AP, RRID: AB_10700003), mouse monoclonal anti-Tuj1 (1:5000, Proteintech, Cat# 66375-1-Ig, RRID: AB_2814998), rabbit polyclonal anti-Bax (1:5000, Proteintech, Cat# 50599-2-Ig, RRID: AB_2061561), rabbit polyclonal anti-cleaved-caspase-3 (1:500, Abcam, Cat# ab2302, RRID: AB_302962), and rabbit polyclonal anti-GAPDH (1:5000, Proteintech, Cat# 10494-1-AP, RRID: AB_2263076). The membrane was then washed three times with TBST solution and incubated with diluted secondary antibody (goat anti-rabbit IgG [1:10,000, Abcam, Cat# ab6721, RRID: AB_955447] and goat anti-mouse IgG [1:8000, Abcam, Cat# ab6789, RRID: AB_955439]) for 1 hour at room temperature. Images were acquired using a MiniChemi 580 chemiluminescence imager (Sage Creation, Beijing, China), and the density of each band was semi-quantified using ImageJ software (National Institutes of Health, Bethesda, MD, USA).

Statistical analysis
All data are expressed as the mean with error bars representing standard deviation (SD). Multiple comparisons were performed using one-way analysis of variance (ANOVA) and Tukey's *post hoc* test. Data were calculated by GraphPad Prism 7.0 software (GraphPad Software, San Diego, CA, USA, www.graphpad.com). $P < 0.05$ was considered statistically significant.

Results

Characterization of hNSCs and hNSC-Exo
hNSCs grow in cell suspension and can form large neurospheres when cultured for 5–7 days. We used immunofluorescence to observe free single cells and neurospheres and confirmed that the NSC markers nestin and Sox2 were expressed (**Figure 1A**). Under induction with differentiation medium, NSCs were observed to differentiate into oligodendrocytes (identified by the marker MOG), neurons (Tuj1), and astrocytes (GFAP).

BDNF protein was encapsulated into neural stem cell-derived exosomes. Pure nanoparticles from the culture supernatant of hNSCs (hNSC-Exo and BDNF-hNSC-Exo) were evaluated by TEM, NTA, and western blotting. TEM revealed that the nanoparticles showed the typical cup-shaped exosome morphology (**Figure 1B**). NTA indicated that the diameter of the particles ranges from 50 to 150 nm (**Figure 1C**). Western blotting revealed the expression of typical exosome markers such as CD81, HSP70, and TSG101, whereas the calnexin negative control was not expressed (**Figure 1D**). Therefore, these isolated vesicles were considered to be hNSC-Exo. Notably, the diameter of exosomes did not change after encapsulating BDNF. These results suggest that BDNF loading does not affect the characteristics of exosomes derived from hNSCs. We also used exosomes for cell tracing *in vitro*. PKH67-labeled exosomes accumulated around the nucleus of target cells, and the entrapment of BDNF did not affect the uptake into target cells (**Figure 1E**).

BDNF-hNSC-Exo reduces apoptosis in the H_2O_2 stress model
Oxidative stress is one of the key pathogenic mechanisms of nerve apoptosis and neurological dysfunction in ischemic stroke (Belayev et al., 2017; Lai et al., 2020). We used H_2O_2 to induce oxidative damage in NSCs. We transfected BDNF-hNSC-Exo into NSCs treated with H_2O_2, and western blotting confirmed the expression of BDNF in target cells transfected with BDNF-hNSC-Exo (**Figure 2A**).

qRT-PCR, western blotting, and immunofluorescence staining showed that both BDNF-hNSC-Exo and hNSC-Exo promoted the differentiation of NSCs into neurons, and the differentiation ability of the BDNF-hNSC-Exo group was better than that of the hNSC-Exo group (**Figure 2B–D**).

CCK8, TUNEL, and western blotting were performed to evaluate the effect of exosomes on NSCs treated with H_2O_2. CCK8 assay showed that BDNF-hNSC-Exo exhibited a higher cell viability under oxidative stress (**Figure 2E**). Similar results were found using TUNEL staining. As shown in **Figure 2F**, the TUNEL-positive rate was lower in both hNSC-Exo and BDNF-hNSC-Exo groups compared with the PBS control group. However, BDNF-hNSC-Exo could greatly enhance the survival of NSCs compared to hNSC-Exo alone. The expression of Bax and cleaved-caspase-3 was detected by western blotting to assess apoptosis. The BDNF-hNSC-Exo-treated cells showing lower apoptosis in response to H_2O_2 and reduced induction of Bax and cleaved caspase 3 (**Figure 2G**).

BDNF-hNSC-Exo treatment improves neurological function after ischemic stroke and reduces infarct volume
We next evaluated the therapeutic effect of BDNF-hNSC-Exo after stroke using a MCAO rat model (**Figure 3A**). To establish the MCAO model, the common carotid artery and external carotid artery on one side of the rat were ligated, and the suture was inserted into the middle cerebral artery for 90 minutes. BDNF-hNSC-Exo, hNSC-Exo or PBS was injected into the striatal region of cerebral ischemic stroke rats 3 days after stroke (n = 15 animals/group). As expected, compared with the hNSC-Exo and PBS groups, the BDNF-hNSC-Exo-injected rats showed increased BDNF expression in the brain tissue at 28 days after treatment (**Figure 3B**).

We used rotarod, mNSS, and postural reflex tests to evaluate the neurological function of rats with cerebral ischemia before modeling and 28 days after transplantation (**Figure 3C–E**). The neurological function of the BDNF-hNSC-Exo group and the hNSC-Exo group was markedly improved four weeks after transplantation compared with the PBS control group, and the BDNF-hNSC-Exo group performed better than hNSC-Exo group. In addition, the results of TTC staining showed that the infarct volumes of the BDNF-hNSC-Exo group and the hNSC-Exo group were significantly smaller than that of the PBS control group (**Figure 3F**).

BDNF-hNSC-Exo treatment promotes tissue repair in the ischemic model rats
The rate of BrdU/Tuj1 and BrdU/GFAP double-positive cells was evaluated in the peri-infarct zone. Immunofluorescence staining showed that there were more BrdU/Tuj1 double-positive cells around the infarct area in the BDNF-hNSC-Exo and hNSC-Exo groups compared with the PBS group, indicating that more functional neurons were produced (**Figure 4A**). The percentage of BrdU/GFAP double positive cells around the ischemic area was lower in the hNSC-Exo group and the BDNF-hNSC-Exo group than in the PBS group (**Figure 4B**). To evaluate the inflammatory response of BDNF-hNSC-Exo to the brain after cerebral ischemia, the rate of Iba-1-positive cells near the injury site was evaluated using immunofluorescence. The results confirmed that BDNF-hNSC-Exo significantly inhibited the activation of microglia (**Figure 4C**).

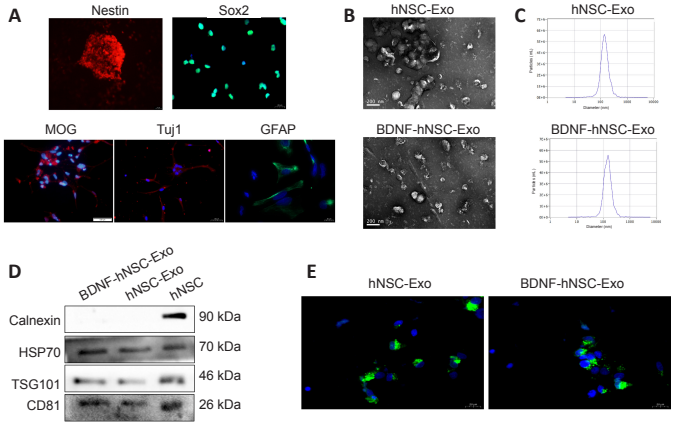

Figure 1 | The features of hNSCs and engineered exosomes (Exo).
(A) Immunofluorescence showed the expression of Nestin (red), Sox2 (green), MOG (red), Tuj1 (red), and GFAP (green). Nuclei were stained by DAPI (blue). Scale bars: 100 μm in the MOG panel; 50 μm in the Tuj1 panel; 20 μm in Nestin, Sox2 and GFAP panels. (B) hNSC-Exo and BDNF-hNSC-Exo showed cup-shaped exosome morphology under TEM. Scale bars: 200 μm. (C) NTA analysis indicated a similar size range for hNSC-Exo and BDNF-hNSC-Exo. (D) Western blot analysis of exosomal marker proteins including CD81, HSP70, and TSG101 and calnexin (as a negative control). (E) Representative micrographs of exosome uptake in NSCs incubated with PKH67-labeled exosomes (green) for 48 hours. Nuclei were stained by DAPI (blue). Scale bars: 20 μm. BDNF: Brain-derived neurotrophic factor; GFAP: glial fibrillary acidic protein; hNSC: human neural stem cell; HSP70: heat shock protein 70; MOG: myelin oligodendrocyte glycoprotein; TSG101: tumor susceptibility 101; Tuj1: β-tubulin III.

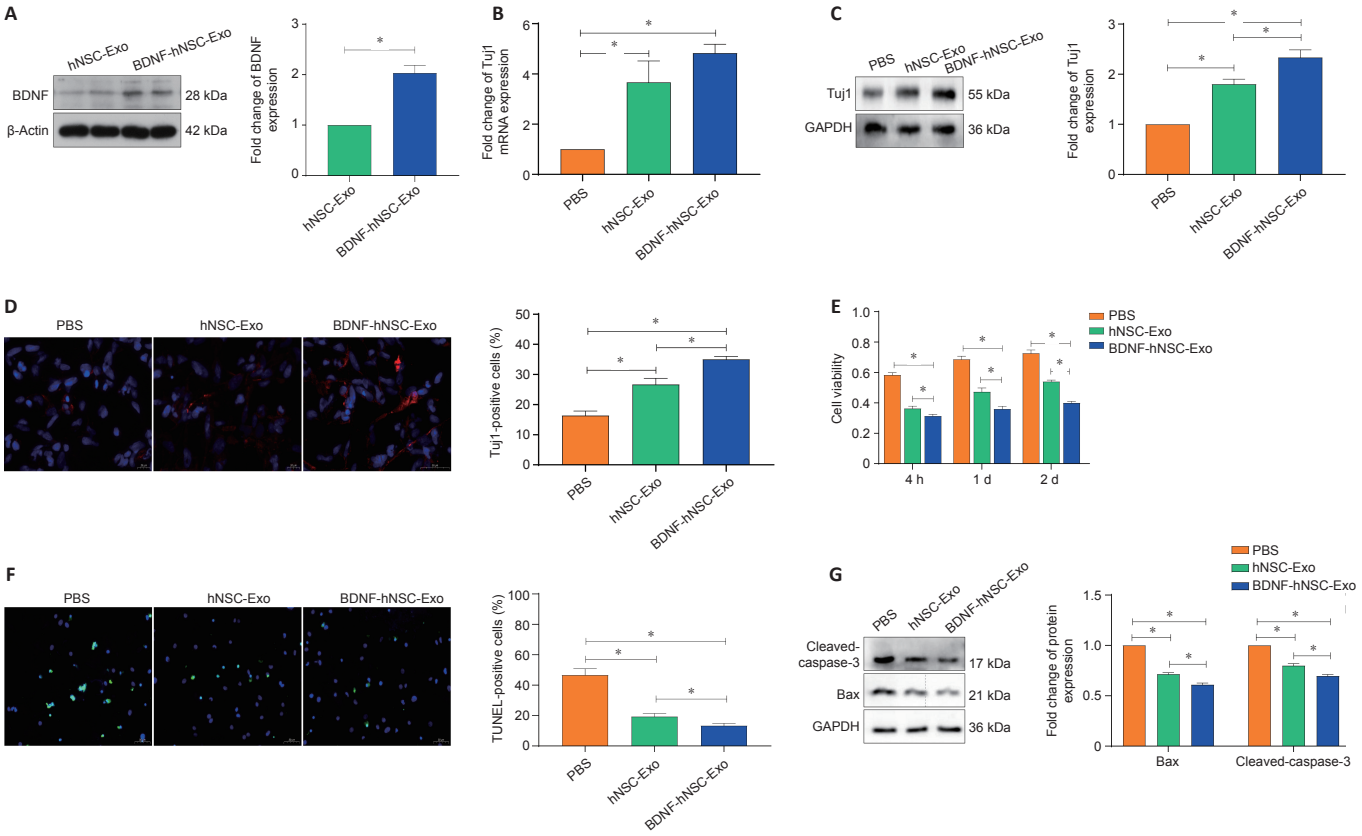

Figure 2 | BDNF-hNSC-Exo promotes the survival and differentiation of neural stem cells *in vitro*.
(A) The expression level of BDNF was measured by western blotting after the addition of BDNF-hNSC-Exo to cultured neural stem cells. Data were normalized to β-actin expression. (B) The differentiation efficiency of BDNF-hNSC-Exo was evaluated using quantitative reverse transcription-polymerase chain reaction. Data were normalized to GAPDH mRNA expression. Cells were treated with a 500 μM solution H_2O_2 for 5 hours. (C) Western blot analysis of Tuj1 in neural stem cells. Cells were treated with a 500 μM solution H_2O_2 for 5 hours. Data were normalized to GAPDH expression. (D) Immunofluorescence showed that the ratio of Tuj1-positive cells (red) in the BDNF-hNSC-Exo group was higher than that in the control group. The percentage of Tuj1-positive cells was obtained by counting cells in three visual fields. Cells were treated with a 500 μM solution H_2O_2 for 5 hours. Nuclei were stained by DAPI (blue). Scale bars: 50 μm. (E) BDNF-hNSC-Exo remarkably increased cell survival in the H_2O_2 stress model (CCK8 assay). Cells were treated with a 500 μM solution H_2O_2 for 5 hours. (F) TUNEL-positive cells. The proportion of TUNEL-positive cells in the BDNF-hNSC-Exo group was remarkably lower than that in the PBS group. Cells were treated with a 500 μM solution H_2O_2 for 5 hours. Nuclei were stained by DAPI (blue). Scale bars: 50 μm. (G) Western blotting showed that the expressions of apoptosis-related proteins cleaved-caspase-3 and Bax were significantly decreased in the BDNF-hNSC-Exo group compared with the other two groups. Cells were treated with a 500 μM solution H_2O_2 for 5 hours. Data were normalized to GAPDH expression. All experiments were conducted in triplicate. All data are presented as mean ± SEM. *$P < 0.05$ (one-way analysis of variance followed by Tukey's *post hoc* test). Bax: Bcl2 associated X, apoptosis regulator; BDNF: brain-derived neurotrophic factor; Exo: exosomes; GAPDH: glyceraldehyde-3-phosphate dehydrogenase; hNSC: human neural stem cell; Tuj1: β-tubulin III.

Discussion

In this study, we found that BDNF-hNSC-Exo attenuated NSCs stress injury and promoted the differentiation of NSCs into neurons. BDNF-hNSC-Exo also inhibited inflammation, thereby creating a suitable immune microenvironment for nerve regeneration.

Although BDNF has emerged as a promising contender for new strategies for stroke treatment, the vast majority of small molecule drugs and biomacromolecules have poor brain bioavailability (Ahmad et al., 2022). Recent studies have shown that exosomes have advantages in their ability to cross biological barriers and their high biocompatibility. Exosomes fuse with the recipient cell membrane to deliver their contents to the recipient cells (Kalluri and LeBleu, 2020). In this study, we used NSC-derived exosomes as delivery vehicles to improve the bioavailability of BDNF. Our results confirmed that BDNF-hNSC-Exo showed standard vesicle shape and diameter, and NTA and TEM revealed no difference in the shape and density between hNSC-Exo and BDNF-hNSC-Exo. In addition, there was no significant difference between BDNF-hNSC-Exo and hNSC-Exo uptake by hNSCs. These results confirmed that BDNF loading did not affect the native properties of exosomes and that BDNF could be efficiently internalized into NSCs. The survival rate of NSCs is reduced in the harsh ischemic microenvironment (Kriegstein and Alvarez-Buylla, 2009). We found that BDNF-hNSC-Exo protected NSCs against H_2O_2-induced damage and greatly enhanced cell survival. In addition, BDNF-hNSC-Exo reduced

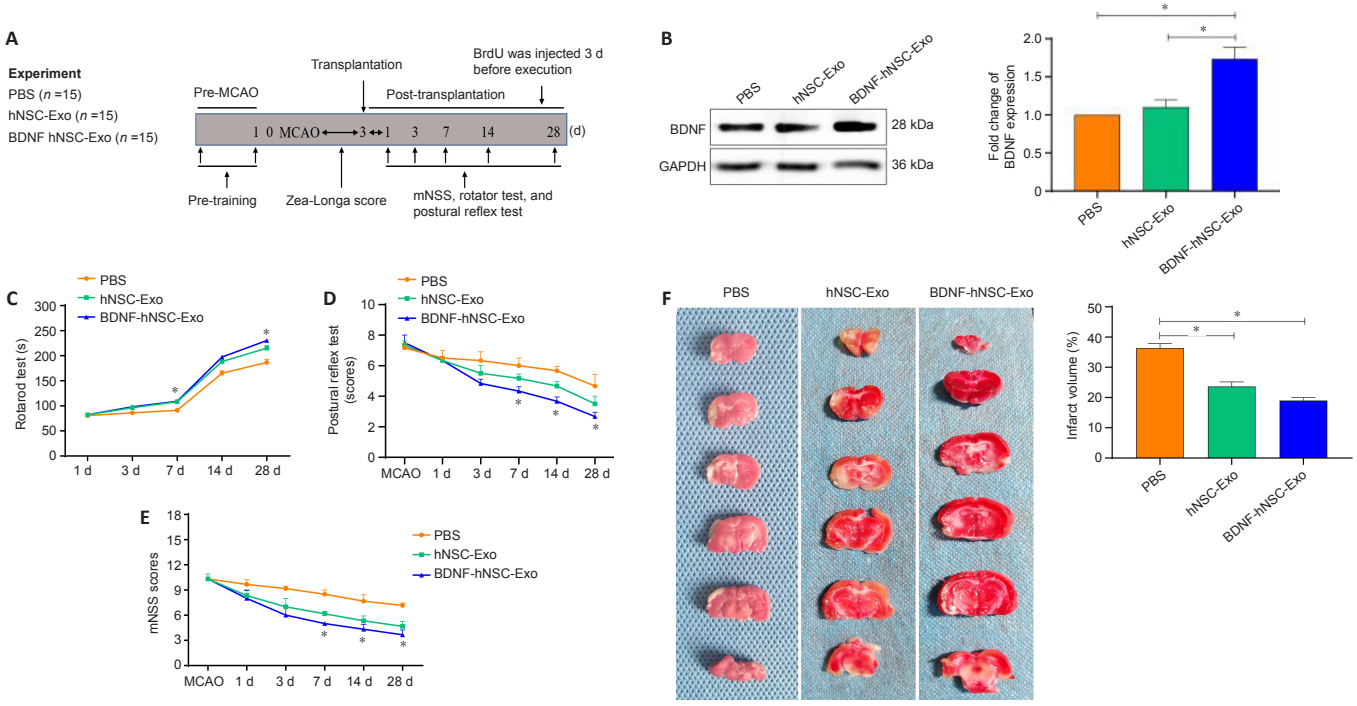

Figure 3 | **BDNF-hNSC-Exo improves neurological deficits and brain damage in rats following cerebral ischemia.**
(A) Experimental design. (B) BDNF-hNSC-Exo increases the expression of BDNF in the infarct areas. Data were normalized to GAPDH expression. (C–E) Evaluation of the behavioral function of MCAO rats at 1, 3, 7, 14, and 28 days after BDNF-hNSC-Exo treatment by rotarod, postural reflex, and mNSS tests. n = 7–10 rats/group. (F) TTC staining showed that BDNF-hNSC-Exo significantly reduced the volume of cerebral infarction. White indicates infact region. n = 3 rats/group. All data are mean ± SEM. *P < 0.05 (one-way analysis of variance followed by Tukey's *post hoc* test). BDNF: Brain-derived neurotrophic factor; Exo: exosomes; GAPDH: glyceraldehyde-3-phosphate dehydrogenase; hNSC: human neural stem cell; MCAO: middle cerebral artery occlusion; mNSS: modified neurological severity score; PBS: phosphate-buffered saline; TTC: 2,3,5-triphenyltetrazolium chloride.

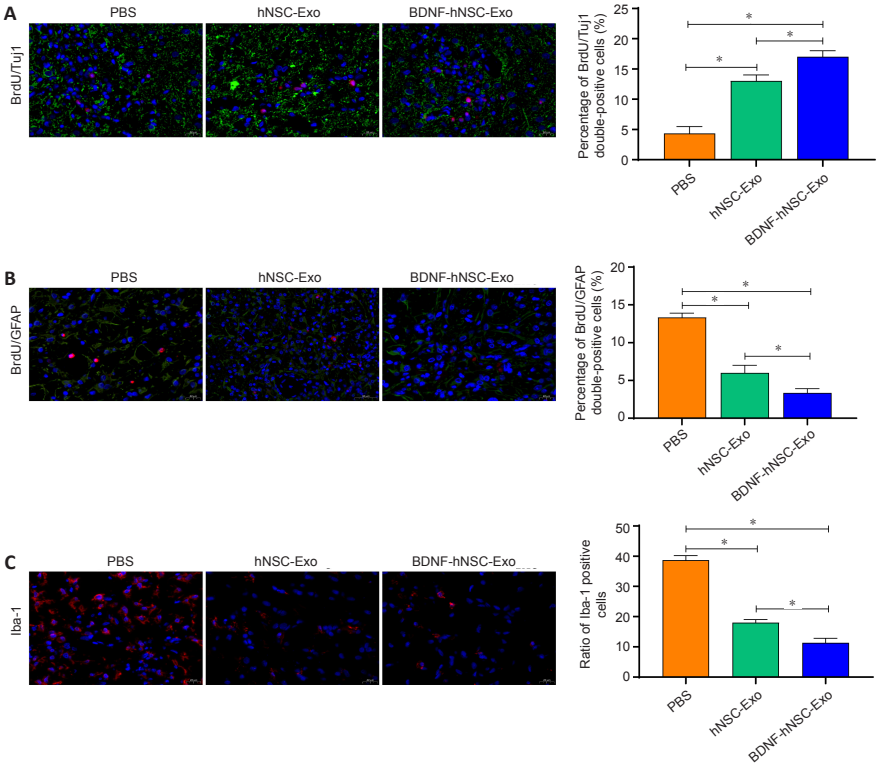

Figure 4 | **BDNF-hNSC-Exo inhibit neuroinflammation and promote neurogenesis in the peri-infarct zone of rats.**
(A) Immunofluorescence double-labeling demonstrated that more functional neurons in the peri-infarct area were generated in the BDNF-hNSC-Exo and hNSC-Exo groups than in the PBS group. BrdU (red) co-localized with Tuj1 (green). Nuclei were stained by DAPI (blue). Scale bar: 20 μm. n = 5 rats/group. (B) Double immunofluorescence staining showed that in the BDNF-hNSC-Exo group, the proportion of BrdU/GFAP double-positive cells in the peri-infarct area was lower than that in the hNSC-Exo group and the PBS group on day 28 after treatment. BrdU (red) co-localized with GFAP (green). Nuclei were stained by DAPI (blue). Scale bar: 20 μm. n = 5 rats/group. (C) Immunofluorescence showed that BDNF-hNSC-Exo significantly reduced the expression of Iba1 (red), indicating reduced neuroinflammation. Nuclei were stained by DAPI (blue). Scale bar: 20 μm. n = 5 rats/group. All data are shown as the mean ± SEM. *P < 0.05 (one-way analysis of variance followed by Tukey's *post hoc* test). BDNF: Brain-derived neurotrophic factor; BrdU: bromodeoxyuridine; Exo: exosomes; GFAP: glial fibrillary acidic protein; hNSC: human neural stem cell; Iba1: induction of brown adipocytes 1; MCAO: middle cerebral artery occlusion; PBS: phosphate-buffered saline; Tuj1: β-tubulin.

apoptosis of NSCs and inhibited the expression of apoptosis-related markers caspase-3 and Bax. Most endogenous NSCs undergo apoptosis in response to hypoxia, oxidative stress, and inflammation (Song et al., 2013; Zhang and Chopp, 2016a). We speculate that BDNF-hNSC-Exo promotes the recovery of neurological function after cerebral ischemia, at least in part, by inhibiting the apoptosis of NSCs.

NSCs have been shown to be helpful in the treatment of various neuropathological diseases (Lv et al., 2021; Peruzzotti-Jametti et al., 2021), including stroke (Hamblin et al., 2022). Previous studies have revealed the proliferation and differentiation of NSCs in the ventricle of MCAO model rats (Li and Clevers, 2010). However, the effects of hypoxia on endogenous NSCs leads to inhibition of neuronal differentiation in the process of self-repair, which in turn affects neural network remodeling after ischemia (Kriegstein and Alvarez-Buylla, 2009). Our study revealed more BrdU/Tuj1 double-positive cells around the cerebral ischemic area of the BDNF-hNSC-Exo group, indicating that BDNF-hNSC-Exo significantly promote the differentiation of hypoxic NSCs into neurons, which is consistent with the *in vitro* results. Although the present study found that the proportion of BrdU/GFAP double-positive cells in the cerebral ischemic area was decreased in both BDNF-hNSC-Exo and hNSC-Exo groups, our results did not rule out that this was caused by

BrdU-labeled proliferating astrocytes. Therefore, further studies are needed to determine whether hNSC-Exo and BDNF-hNSC-Exo inhibit the differentiation of hypoxic NSCs into astrocytes.

Microglia are the resident innate immune cells of the central nervous system that first respond to damage to the central nervous system (Xiong et al., 2016). Activated microglia release pro-inflammatory factors, including IL-1β, TNF-α, and IL-6, and recruit peripheral immune cells to cause secondary neuroinflammation (Tian et al., 2021). Our results showed that BDNF-hNSC-Exo significantly inhibited the activation of microglia, suppressed neuroinflammatory responses, and improved the immune microenvironment, thereby creating favorable conditions for nerve regeneration. This result suggests that BDNF-hNSC-Exo may exert therapeutic effects by altering the immune response.

Overall, these data indicate that BDNF-hNSC-Exo promote nerve regeneration and reduce the neuroinflammatory response after cerebral ischemia. However, this study has some limitations. Given the poor targeting of exosomes, we used a stereotaxic injection method, which is invasive. Furthermore, although our results help illuminate the function of BDNF-hNSC-Exo, the underlying mechanisms of BDNF-hNSC-Exo remain unclear and more studies are needed to determine the mechanisms.

Conclusion

We successfully prepared an engineered exosomes from NSCs loaded with BDNF to reduce the damage caused by cerebral ischemia. Compared with hNSC-Exo, BDNF-hNSC-Exo showed enhanced anti-apoptosis and differentiation-promoting ability. The finding revealed that BDNF-hNSC-Exo substantially lowered the apoptosis of hNSCs intervened by exposure to H_2O_2, and promoted the differentiation of hNSC into neurons. In the rat ischemic stroke model, compared with hNSC-Exo, in addition to promoting the differentiation of endogenous NSCs into neurons, BDNF-hNSC-Exo effectively inhibited the expression of microglia, thereby reducing inflammation. Due to these therapeutic effects, BDNF-hNSC-Exo resulted in reduced infarct volume and improved neurological function. In summary, these results indicate that engineered exosomes may be a potentially effective repair strategy in the treatment of ischemic stroke injury.

Author contributions: *Study design: ZHZ and LKC; manuscript writing: ZHZ, WA and LKC; experimental operation: ZHZ, FJ, WA, GLZ, HW, CQL and WHC; statistical analysis: ZHZ and LKC; final review: ZHZ and LKC. All the authors approved the final version of the manuscript.*

Conflicts of interest: *The authors declare no conflict of interest.*

References

Ahmad J, Haider N, Khan MA, Md S, Alhakamy NA, Ghoneim MM, Alshehri S, Sarim Imam S, Ahmad MZ, Mishra A (2022) Novel therapeutic interventions for combating Parkinson's disease and prospects of Nose-to-Brain drug delivery. Biochem Pharmacol 195:114849.

Arumugam TV, Chan SL, Jo DG, Yilmaz G, Tang SC, Cheng A, Gleichmann M, Okun E, Dixit VD, Chigurupati S, Mughal MR, Ouyang X, Miele L, Magnus T, Poosala S, Granger DN, Mattson MP (2006) Gamma secretase-mediated Notch signaling worsens brain damage and functional outcome in ischemic stroke. Nat Med 12:621-623.

Belayev L, Mukherjee PK, Balaszczuk V, Calandria JM, Obenaus A, Khoutorova L, Hong SH, Bazan NG (2017) Neuroprotectin D1 upregulates Iduna expression and provides protection in cellular uncompensated oxidative stress and in experimental ischemic stroke. Cell Death Differ 24:1091-1099.

Chen W, Wang H, Zhu Z, Feng J, Chen L (2020) Exosome-shuttled circSHOC2 from IPASs regulates neuronal autophagy and ameliorates ischemic brain injury via the miR-7670-3p/SIRT1 axis. Mol Ther Nucleic Acids 22:657-672.

Fang SB, Zhang HY, Wang C, He BX, Liu XQ, Meng XC, Peng YQ, Xu ZB, Fan XL, Wu ZJ, Chen D, Zheng L, Zheng SG, Fu QL (2020) Small extracellular vesicles derived from human mesenchymal stromal cells prevent group 2 innate lymphoid cell-dominant allergic airway inflammation through delivery of miR-146a-5p. J Extracell Vesicles 9:1723260.

Feng J, Zhang Y, Zhu Z, Gu C, Waqas A, Chen L (2021) Emerging exosomes and exosomal miRNAs in spinal cord injury. Front Cell Dev Biol 9:703989.

Fu W, Lei C, Liu S, Cui Y, Wang C, Qian K, Li T, Shen Y, Fan X, Lin F, Ding M, Pan M, Ye X, Yang Y, Hu S (2019) CAR exosomes derived from effector CAR-T cells have potent antitumour effects and low toxicity. Nat Commun 10:4355.

Goldstein LB (2007) Acute ischemic stroke treatment in 2007. Circulation 116:1504-1514.

Hamblin MH, Murad R, Yin J, Vallim G, Lee JP (2022) Modulation of gene expression on a transcriptome-wide level following human neural stem cell transplantation in aged mouse stroke brains. Exp Neurol 347:113913.

Hao Y, Xiong R, Gong X (2021) Memantine, NMDA receptor antagonist, attenuates ox-LDL-induced inflammation and oxidative stress via activation of BDNF/TrkB signaling pathway in HUVECs. Inflammation 44:659-670.

Huang F, Chen T, Chang J, Zhang C, Liao F, Wu L, Wang W, Yin Z (2021) A conductive dual-network hydrogel composed of oxidized dextran and hyaluronic-hydrazide as BDNF delivery systems for potential spinal cord injury repair. Int J Biol Macromol 167:434-445.

Hughes D, Judge C, Murphy R, Loughlin E, Costello M, Whiteley W, Bosch J, O'Donnell MJ, Canavan M (2020) Association of blood pressure lowering with incident dementia or cognitive impairment: a systematic review and meta-analysis. Jama 323:1934-1944.

Kalluri R, LeBleu VS (2020) The biology, function, and biomedical applications of exosomes. Science 367:eaau6977.

Kim H, Kim EH, Kwak G, Chi SG, Kim SH, Yang Y (2020) Exosomes: cell-derived nanoplatforms for the delivery of cancer therapeutics. Int J Mol Sci 22:14.

Kriegstein A, Alvarez-Buylla A (2009) The glial nature of embryonic and adult neural stem cells. Annu Rev Neurosci 32:149-184.

Lai Y, Lin P, Chen M, Zhang Y, Chen J, Zheng M, Liu J, Du H, Chen R, Pan X, Liu N, Chen H (2020) Restoration of L-OPA1 alleviates acute ischemic stroke injury in rats via inhibiting neuronal apoptosis and preserving mitochondrial function. Redox Biol 34:101503.

Leira EC, Russman AN, Biller J, Brown DL, Bushnell CD, Caso V, Chamorro A, Creutzfeldt CJ, Cruz-Flores S, Elkind MSV, Fayad P, Froehler MT, Goldstein LB, Gonzales NR, Kaskie B, Khatri P, Livesay S, Liebeskind DS, Majersik JJ, Moheet AM, et al. (2020) Preserving stroke care during the COVID-19 pandemic: Potential issues and solutions. Neurology 95:124-133.

Li L, Clevers H (2010) Coexistence of quiescent and active adult stem cells in mammals. Science 327:542-545.

Li Z, Wang H, Xiao G, Du H, He S, Feng Y, Zhang B, Zhu Y (2021) Recovery of post-stroke cognitive and motor deficiencies by Shuxuening injection via regulating hippocampal BDNF-mediated neurotrophin/Trk signaling. Biomed Pharmacother 141:111828.

Lv ZY, Li Y, Liu J (2021) Progress in clinical trials of stem cell therapy for cerebral palsy. Neural Regen Res 16:1377-1382.

Ma Q, Li R, Wang L, Yin P, Wang Y, Yan C, Ren Y, Qian Z, Vaughn MG, McMillin SE, Hay SI, Naghavi M, Cai M, Wang C, Zhang Z, Zhou M, Lin H, Yang Y (2021) Temporal trend and attributable risk factors of stroke burden in China, 1990-2019: an analysis for the Global Burden of Disease Study 2019. Lancet Public Health 6:e897-906.

Marko M, Posekany A, Szabo S, Scharer S, Kiechl S, Knoflach M, Serles W, Ferrari J, Lang W, Sommer P, Greisenegger S (2020) Trends of r-tPA (recombinant tissue-type plasminogen activator) treatment and treatment-influencing factors in acute ischemic stroke. Stroke 51:1240-1247.

Muheremu A, Shu L, Liang J, Aili A, Jiang K (2021) Sustained delivery of neurotrophic factors to treat spinal cord injury. Transl Neurosci 12:494-511.

Naqvi S, Panghal A, Flora SJS (2020) Nanotechnology: a promising approach for delivery of neuroprotective drugs. Front Neurosci 14:494.

Paxinos G, Watson C (2009) The rat brain in stereotaxic coordinates. San Diego: Elsevier Academic Press.

Percie du Sert N, Hurst V, Ahluwalia A, Alam S, Avey MT, Baker M, Browne WJ, Clark A, Cuthill IC, Dirnagl U, Emerson M, Garner P, Holgate ST, Howells DW, Karp NA, Lazic SE, Lidster K, MacCallum CJ, Macleod M, Pearl EJ, et al. (2020) The ARRIVE guidelines 2.0: Updated guidelines for reporting animal research. PLoS Biol 18:e3000410.

Peruzzotti-Jametti L, Bernstock JD, Willis CM, Manferrari G, Rogall R, Fernandez-Vizarra E, Williamson JC, Braga A, van den Bosch A, Leonardi T, Krzak G, Kittel Á, Benincá C, Vicario N, Tan S, Bastos C, Bicci I, Iraci N, Smith JA, Peacock B, et al. (2021) Neural stem cells traffic functional mitochondria via extracellular vesicles. PLoS Biol 19:e3001166.

Song J, Cho KJ, Cheon SY, Kim SH, Park KA, Lee WT, Lee JE (2013) Apoptosis signal-regulating kinase 1 (ASK1) is linked to neural stem cell differentiation after ischemic brain injury. Exp Mol Med 45:e69.

Tian T, Cao L, He C, Ye Q, Liang R, You W, Zhang H, Wu J, Ye J, Tannous BA, Gao J (2021) Targeted delivery of neural progenitor cell-derived extracellular vesicles for anti-inflammation after cerebral ischemia. Theranostics 11:6507-6521.

Vogel A, Upadhya R, Shetty AK (2018) Neural stem cell derived extracellular vesicles: Attributes and prospects for treating neurodegenerative disorders. EBioMedicine 38:273-282.

Wu P, Zhang B, Ocansey DKW, Xu W, Qian H (2021) Extracellular vesicles: A bright star of nanomedicine. Biomaterials 269:120467.

Xiong LL, Chen J, Du RL, Liu J, Chen YJ, Hawwas MA, Zhou XF, Wang TH, Yang SJ, Bai X (2021) Brain-derived neurotrophic factor and its related enzymes and receptors play important roles after hypoxic-ischemic brain damage. Neural Regen Res 16:1453-1459.

Xiong XY, Liu L, Yang QW (2016) Functions and mechanisms of microglia/macrophages in neuroinflammation and neurogenesis after stroke. Prog Neurobiol 142:23-44.

Xu X, Liang Y, Li X, Ouyang K, Wang M, Cao T, Li W, Liu J, Xiong J, Li B, Xia J, Wang D, Duan L (2021) Exosome-mediated delivery of kartogenin for chondrogenesis of synovial fluid-derived mesenchymal stem cells and cartilage regeneration. Biomaterials 269:120539.

Yuan D, Zhao Y, Banks WA, Bullock KM, Haney M, Batrakova E, Kabanov AV (2017) Macrophage exosomes as natural nanocarriers for protein delivery to inflamed brain. Biomaterials 142:1-12.

Yuan P, Ding L, Chen H, Wang Y, Li C, Zhao S, Yang X, Ma Y, Zhu J, Qi X, Zhang Y, Xia X, Zheng JC (2021) Neural stem cell-derived exosomes regulate neural stem cell differentiation through miR-9-Hes1 axis. Front Cell Dev Biol 9:601600.

Zhang G, Chen L, Chen W, Li B, Yu Y, Lin F, Guo X, Wang H, Wu G, Gu B, Miao W, Kong J, Jin X, Yi G, You Y, Su X, Gu N (2018) Neural stem cells alleviate inflammation via neutralization of IFN-γ negative effect in ischemic stroke model. J Biomed Nanotechnol 14:1178-1188.

Zhang G, Zhu Z, Wang H, Yu Y, Chen W, Waqas A, Wang Y, Chen L (2020) Exosomes derived from human neural stem cells stimulated by interferon gamma improve therapeutic ability in ischemic stroke model. J Adv Res 24:435-445.

Zhang Y, Deng H, Pan C, Hu Y, Wu Q, Liu N, Tang Z (2016) Mesenchymal stromal cell therapy in ischemic stroke. J Neurorestoratol 4:79-83.

Zhang Y, Shan Z, Zhao Y, Ai Y (2019) Sevoflurane prevents miR-181a-induced cerebral ischemia/reperfusion injury. Chem Biol Interact 308:332-338.

Zhang Z, Chopp M (2016a) Neural stem cells and ischemic brain. J Stroke 18:267-272.

Zhang ZG, Chopp M (2016b) Exosomes in stroke pathogenesis and therapy. J Clin Invest 126:1190-1197.

Zhong D, Cao Y, Li CJ, Li M, Rong ZJ, Jiang L, Guo Z, Lu HB, Hu JZ (2020) Neural stem cell-derived exosomes facilitate spinal cord functional recovery after injury by promoting angiogenesis. Exp Biol Med (Maywood) 245:54-65.

C-Editor: Zhao M; S-Editor: Li CH; L-Editors: Wolf GW, Li CH, Song LP; T-Editor: Jia Y